Chelate-Ring-Dependent Shifts in Redox Isomerism for the $Co(Me_2N(CH_2)_nNMe_2)(3,6\text{-}DBQ)_2$ ($n = 1-3$) Series, Where 3,6-DBQ Is the Semiquinonate or Catecholate Ligand Derived from 3,6-Di-*tert*-butyl-1,2-benzoquinone

Ok-Sang Jung,*[,1a] Du Hwan Jo,[1a] Young-A Lee,[1a] Youn Soo Sohn,[1a] and Cortlandt G. Pierpont*[,1b]

Korea Institute of Science and Technology, Cheongryang, Seoul, 130-650 South Korea, and Department of Chemistry and Biochemistry, University of Colorado, Boulder, Colorado 80309

Received May 13, 1998

Intramolecular electron transfer between $Co^{II}(SQ)$ and $Co^{III}(Cat)$ redox isomers has been investigated for the series of complexes $Co(N\text{-}N)(3,6\text{-}DBQ)_2$, where 3,6-DBQ is the semiquinonate or catecholate form of 3,6-di-*tert*-butyl-1,2-benzoquinone and N-N is tetramethylmethylenediamine (tmmda), tetramethylethylenediamine (tmeda), or tetramethylpropylenediamine (tmpda). Measurements of magnetic properties and changes in electronic spectra indicate that the transition temperature ($T_{1/2}$) for Co(III)/Co(II) redox isomerism in the solid state and in toluene solution is the lowest for $Co(tmpda)(3,6\text{-}DBQ)_2$. This is attributed to the flexibility of the six-membered chelate ring of Co(tmpda) and a positive contribution to ΔS for the equilibrium. Transition temperatures for the tmmda and tmeda analogues are more than 150 deg higher than that for the tmpda species. Structural characterization of $Co^{III}(tmmda)(3,6\text{-}DBSQ)(3,6\text{-}DBCat)$, $Co^{III}(tmeda)(3,6\text{-}DBSQ)(3,6\text{-}DBCat)$, and $Co^{II}(tmpda)(3,6\text{-}DBSQ)_2$ has shown that the Co(tmmda) and Co(tmeda) chelate rings are conformationally ordered, while there is considerable disorder in the Co(tmpda) chelate ring. In toluene solution, $T_{1/2}$ is approximately 15 deg higher for $Co(tmeda)(3,6\text{-}DBSQ)_2$ than for the tmmda analogue due to the more contracted chelate ring of $Co^{III}(tmmda)(3,6\text{-}DBSQ)(3,6\text{-}DBCat)$. For the $Co(N\text{-}N)(3,6\text{-}DBQ)_2$ series, $T_{1/2}$ varies as tmpda $\ll$ tmmda $<$ tmeda.

Introduction

Several years ago we reported the equilibrium between Co(III) and Co(II) redox isomers of a complex containing semiquinonate (SQ) and catecholate (Cat) ligands derived from 3,5-di-*tert*-butyl-1,2-benzoquinone (3,5-DBBQ) (eq 1).[2] We referred

$$Co^{III}(bpy)(3,5\text{-}DBSQ)(3,5\text{-}DBCat) \rightarrow Co^{II}(bpy)(3,5\text{-}DBSQ)_2 \quad (1)$$

to this equilibrium as valence tautomerism (VT), following references to equilibria of main group compounds that involve similar shifts in formal oxidation state.[3] While shifts in charge distribution between redox-active metal−ligand combinations may potentially lead to similar equilibria, the quinone complexes of Co and Mn have spectroscopic and structural features indicating charge-localized electronic structures.[4,5] Charge delocalization of the type associated with "noninnocent" ligands such as the 1,2-dithiolenes and diimines is a relatively minor effect for the quinone complexes of first-row transition metal ions.[6]

In recent research, the range of complexes that show VT has been extended to a broad class of N-donor ancillary ligands and to complexes prepared with 3,6-DBBQ.[4,7] Equilibria occur in separate electron transfer (eq 2) and spin transition (eq 3)

$$\underset{(d\pi)^6(d\sigma)^0(\pi_{Q1})^2(\pi_{Q2})^1}{Co^{III}(N\text{-}N)(SQ)(Cat)} \rightarrow \underset{(d\pi)^6(d\sigma)^1(\pi_{Q1})^1(\pi_{Q2})^1}{Co^{II}(N\text{-}N)(SQ)_2} \quad (2)$$

$$\underset{(d\pi)^6(d\sigma)^1(\pi_{Q1})^1(\pi_{Q2})^1}{Co^{II}(N\text{-}N)(SQ)_2} \rightarrow \underset{(d\pi)^5(d\sigma)^2(\pi_{Q1})^1(\pi_{Q2})^1}{Co^{II}(N\text{-}N)(SQ)_2} \quad (3)$$

steps that convert low-spin Co(III) to high-spin Co(II) in a process that may be viewed as a charge-transfer-induced spin transition. Equilibrium measurements on $Co(bpy)(3,5\text{-}DBQ)_2$ and $Co(phen)(3,5\text{-}DBQ)_2$ recorded in solution and in the solid state have provided thermodynamic parameters that are in general agreement with values for intramolecular enthalpy and entropy changes associated with Co(II/III) redox reactions.[8,9] Changes in the population of the antibonding dσ orbital are responsible for the positive changes in entropy and enthalpy that define the transition temperature, $T_{1/2}$. This model also applies to bimodal Mn(IV/III) and Mn(III/II) VT equilibria,[5,10] and it accounts for the absence of redox isomerism for the related complexes of Fe.[11]

(1) (a) Korea Institute of Science and Technology. (b) University of Colorado.
(2) Buchanan, R. M.; Pierpont, C. G. *J. Am. Chem. Soc.* **1980**, *102*, 4951.
(3) Minkin, V. I.; Olekhnovich, L. P.; Zhdanov, Yu. A. *Molecular Design of Tautomeric Compounds*; D. Reidel Publishing Co.: Dordrecht, The Netherlands, 1988.
(4) Jung, O.-S.; Pierpont, C. G. *Inorg. Chem.* **1994**, *33*, 2227.
(5) Attia, A. S.; Pierpont, C. G. *Inorg. Chem.* **1995**, *34*, 1172.
(6) McCleverty, J. A. *Prog. Inorg. Chem.* **1968**, *10*, 49.
(7) (a) Abakumov, G. A.; Cherkasov, V. K.; Bubnov, M. P.; Ellert, O. G.; Dobrokhotova, Z. B.; Zakharov, L. N.; Struchkov, Yu. T. *Dokl. Akad. Nauk SSSR* **1993**, *328*, 12. (b) Adams, D. M.; Dei, A.; Rheingold, A. L.; Hendrickson, D. N. *J. Am. Chem. Soc.* **1993**, *115*, 8221. (c) Jung, O.-S.; Jo, D. H.; Lee, Y.; Conklin, B. J.; Pierpont, C. G. *Inorg. Chem.* **1997**, *36*, 19.
(8) Pierpont, C. G.; Jung, O.-S. *Inorg. Chem.* **1995**, *34*, 4281.
(9) Adams, D. M.; Hendrickson, D. N. *J. Am. Chem. Soc.* **1996**, *118*, 11515.
(10) Attia, A. S.; Pierpont, C. G. *Inorg. Chem.* **1998**, *37*, 3051.

10.1021/ic9805372 CCC: $15.00
Published on Web 10/13/1998

The addition of charge to dσ, or octahedral antibonding e_g, orbitals with the transition from ls-Co(III) to hs-Co(II) results in two fundamental changes within the complex. Bonds to the Co are weakened and increased in length by approximately 0.2 Å, a change that is primarily enthalpic. Associated with weakened Co−L bonds, vibrational modes shift to lower frequency, and isomerism between octahedral and trigonal prismatic coordination geometries may occur. These effects contribute to a relatively large, positive entropy change. In the present study, we have focused specifically on coligand chelate ring flexibility as a feature contributing to ΔS for the VT equilibrium of Co(N-N)(3,6-DBQ)$_2$. Ancillary ligands of the $Me_2N(CH_2)_nNMe_2$ series with $n = 1-3$ have been used to vary the bite angle without an appreciable change in the donation properties of the tertiary amine nitrogens. The sensitivity of $T_{1/2}$ to chelate ring flexibility has been found to be surprisingly high.[12]

Experimental Section

Materials. *N*,*N*,*N*′,*N*′-Tetramethylmethyldiamine (tmmda), *N*,*N*,*N*′,*N*′-tetramethylethylenediamine (tmeda), and *N*,*N*,*N*′,*N*′-tetramethylpropylenediamine (tmpda) were purchased from Aldrich. Dicobalt octacarbonyl was purchased from Strem Chemical Co. 3,6-Di-*tert*-butyl-1,2-benzoquinone (3,6-DBBQ) and Co(tmeda)(3,6-DBSQ)(3,6-DBCat) were prepared using literature procedures.[4,13]

Co(tmmda)(3,6-DBQ)$_2$. $Co_2(CO)_8$ (86 mg, 0.25 mmol) and tmmda (86 mg, 0.50 mmol) were combined in 30 mL of toluene under an atmosphere of Ar. The mixture was stirred for 5 min, and 3,6-DBBQ (220 mg, 1.00 mmol) dissolved in 30 mL of toluene was added. The solution was stirred for 2 h at room temperature. Evaporation of the solvent gave the dark blue microcrystalline product in 75% yield (225 mg). Dark blue crystals of Co(tmmda)(3,6-DBSQ)(3,6-DBCat) suitable for crystallographic characterization were obtained by recrystallization from acetone. Anal. Calcd for $C_{33}H_{54}N_2O_4Co$: C, 65.75; H, 8.96; N, 4.45. Found: C, 65.87; H, 9.05; N, 4.66.

Co(tmpda)(3,6-DBQ)$_2$. The procedure described above was followed, substituting tmpda for tmmda. Co(tmpda)(3,6-DBQ)$_2$ was obtained in 70% yield as dark green crystals. Anal. Calcd for $C_{35}H_{58}N_2O_4Co$: C, 66.42; H, 9.02; N, 4.26. Found: C, 66.75; H, 9.28; N, 4.47.

Physical Measurements. Electronic spectra were recorded on a Perkin-Elmer Lambda 9 spectrophotometer equipped with a RMC-Cyrosystems cryostat. Magnetic measurements were made using a Quantum Design SQUID magnetometer at a field strength of 5 kG. Infrared spectra were recorded on a Perkin-Elmer 1600 FTIR instrument with samples prepared as KBr disks. EPR spectra were recorded on a Bruker ESP-300E spectrometer and referenced to DPPH as the *g* value standard.

Crystallographic Structure Determinations. (a) Co(tmmda)(3,6-DBSQ)(3,6-DBCat). Dark blue crystals of the complex were grown from acetone. Crystals form in the monoclinic crystal system, space group $P2_1/c$, in a unit cell of the dimensions given in Table 1. Intensity data were measured on an Enraf Nonius CAD-4 diffractometer within the angular range in θ of 2.19−24.98°. The Co atom was located on a sharpened Patterson map, and phases generated from the location of the metal gave the positions of other atoms of the structure. Final cycles of refinement converged with discrepancy indices of $R(F) = 0.044$ and $R_w(F^2) = 0.103$.

(b) Co(tmpda)(3,6-DBSQ)$_2$. Dark green crystals were obtained by recrystallization from acetone at room temperature. Crystals form in the monoclinic crystal system, space group $P2_1/c$, in a unit cell of the dimensions listed in Table 1. Intensity data were measured on a Siemens P3F automated diffractometer at room temperature (298 K) and at 150 K. The Co atom was located on a sharpened Patterson map using data collected at room temperature, and phases generated from the location of the metal gave the positions of other atoms of the structure. Rotation about one Co−N bond of the tmpda ligand disordered the methyl and ring propylene carbon atoms. Final cycles of refinement converged with discrepancy indices of $R(F) = 0.080$ and $R_w(F) = 0.100$. To more clearly resolve the disordered locations for the tmpda carbons, a new data set was collected at 150 K. At the lower temperature, locations for the disordered atoms became apparent, but anisotropic refinement resulted in large thermal parameters. Final cycles of refinement carried out with the 150 K data converged with discrepancy indices of $R(F) = 0.074$ and $R_w(F) = 0.105$.

Table 1. Crystallographic Data for Co^{III}(tmmda)(3,6-DBSQ)(3,6-DBCat) and Co^{II}(tmpda)(3,6-DBSQ)$_2$

	Co^{III}(tmmda)(3,6-DBSQ)-(3,6-DBCat)	Co^{II}(tmpda)(3,6-DBSQ)$_2$
formula	$C_{33}H_{54}N_2O_4Co$	$C_{35}H_{59}N_2O_4Co$
fw	601.7	638.8
color	dark blue	dark blue-green
space group	$P2_1/c$	$P2_1/c$
a (Å)	17.916(6)	16.804(2) [16.987(2)][b]
b (Å)	10.525(2)	11.691(2) [11.771(2)][b]
c (Å)	19.174(5)	19.415(3) [19.723(3)][b]
β (deg)	104.51(3)	111.52(1) [111.82(1)][b]
V (Å^3)	3500(2)	3548.3(9) [3661.1(9)][b]
Z	4	4
T (K)	293(2)	150(2)
λ(MoKα) (Å)	0.710 73	0.710 69
D_{calcd} (g cm^{-3})	1.142	1.181 [1.143][b]
μ (mm^{-1})	0.525	0.517 [0.501][b]
R, R_w	0.044, 0.103[a]	0.074, 0.105 [0.080, 0.100][b,c]

[a] $R = \sum||F_o| - |F_c||/\sum|F_o|$; $R_w = [\sum w(F_o^2 - F_c^2)^2/\sum wF_o^4]^{1/2}$. [b] $T =$ 298 K. [c] $R = \sum||F_o| - |F_c||/\sum|F_o|$; $R_w = [\sum w(F_o - F_c)^2/\sum wF_o^2]^{1/2}$.

Tables listing atom positions, anisotropic displacement parameters, and hydrogen atom locations for the three structure determinations are available as Supporting Information.

Results

Thermodynamic changes associated with electron-transfer reactions are the product of contributions from solvation, or outer-sphere effects, and inner-sphere changes in entropy and enthalpy that are more intrinsic to the complex. Studies carried out in fluid solution have been useful in providing information on specific solvent−solute interactions, but separation of intermolecular and intramolecular contributions is difficult. Richardson has used the $Ru(NH_3)_6^{3+/2+}$ redox couple to separate inner- and outer-sphere thermodynamic effects for $Co(NH_3)_6^{3+/2+}$.[14] Intramolecular thermodynamic changes for the $Co^{3+/2+}$ couple are relatively large and consistent with an intuitive ligand-field model. The enthalpy change is positive as a result of weakened Co−L bonds with the change in configuration from low-spin Co(III) to high-spin Co(II). Temperature dependence is associated with a positive entropy change that results from inner-sphere flexibility in coordination geometry and with low-frequency shifts in Co−L vibrations. This simple view ignores contributions from electronic effects, but they are estimated to be relatively small, even with the large change in spin multiplicity for the ls-Co^{III}/hs-Co^{II} couple.[15] Direct experimental observations on inner-sphere thermodynamic changes of redox reactions should, ideally, be made in a solvent-free

(11) Attia, A. S.; Bhattacharya, S.; Pierpont, C. G. *Inorg. Chem.* **1995**, *34*, 4427.
(12) Preliminary results of our characterization on Co(tmpda)(3,6-DBQ)$_2$ were described in a communication: Jung, O.-S.; Jo, D. H.; Lee, Y.; Sohn, Y. S.; Pierpont, C. G. *Angew. Chem., Int. Ed. Engl.* **1996**, *35*, 1694.
(13) Belostotskaya, I. S.; Komissarova, N. L.; Dzhuaryan, E. V.; Ershov, V. V. *Isv. Akad. Nauk SSSR* **1972**, 1594.
(14) Richardson, D. E.; Sharpe, P. *Inorg. Chem.* **1991**, *30*, 1412.
(15) (a) Richardson, D. E.; Sharpe, P. *Inorg. Chem.* **1993**, *32*, 1809. (b) Crawford, P. W.; Schultz, F. A. *Inorg. Chem.* **1994**, *33*, 4344. (c) Gao, Y.-D.; Lipkowitz, K. P.; Schultz, F. A. *J. Am. Chem. Soc.* **1995**, *117*, 11932.

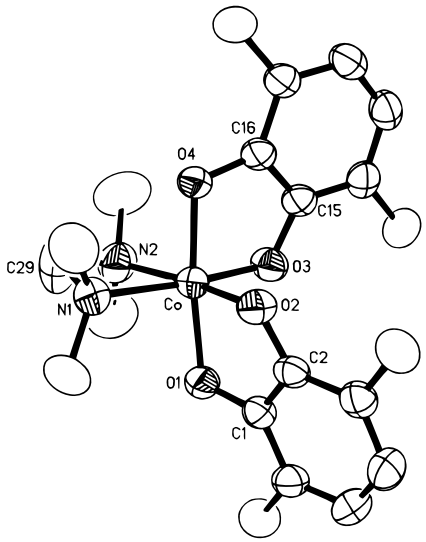

Figure 1. View of the Co^{III}(tmmda)(3,6-DBSQ)(3,6-DBCat) molecule. Oxygens O1 and O2 are associated with the SQ ligand; O3 and O4 are associated with the Cat.

environment. An approach that may be used with success in a solvent medium involves coupling the metal with a redox-active ligand that can transfer an electron reversibly to the metal within the inner coordination sphere under equilibrium conditions. The filled π^* electronic level of the catecholate (Cat) ligand is close in energy to the valence d orbitals of Co(III). The ratio of thermodynamic changes in enthalpy and entropy that occur with the intramolecular shift in charge distribution from ls-Co^{III}(Cat) to hs-Co^{II}(SQ) defines the temperature at which concentrations of both components of the equilibrium are equal, $T_{1/2}$. Ancillary ligands coordinated to the metal influence $T_{1/2}$ through bonding effects; stronger Co−L bonds favor the ls-Co^{III}(Cat) redox isomer.[4] Substituent effects for the bpy and phen ligands of Co^{III}(bpy)(3,6-DBQ)$_2$ and Co^{III}(phen)(3,6-DBQ)$_2$ show this dependence with a decrease in $T_{1/2}$ of approximately 100 deg with the addition of nitro substituents to the diimine ligand ring.[4,16] Chelate ring flexibility may increase the entropy change, decreasing $T_{1/2}$ in favor of the hs-Co^{II}(SQ) isomer. We now report the results of studies on complexes of general form Co(N-N)(3,6-DBQ)$_2$ prepared with tmmda, tmeda, and tmpda, ligands with similar donor properties that differ only in chelate-ring dimension and flexibility.

Co(tmmda)(3,6-DBQ)$_2$. Co(tmmda)(3,6-DBQ)$_2$ was prepared by procedures that are similar to those used to form Co^{III}(tmeda)(3,6-DBSQ)(3,6-DBCat).[4] A crystal obtained by acetone recrystallization was used for a structure determination. The complex molecule is shown in Figure 1; selected bond lengths and angles are listed in Table 2. Values for the Co−O and Co−N bond lengths show clearly that the metal is low-spin Co(III). The average Co−O length of 1.868 Å compares well with 1.872 Å for Co^{III}(tmeda)(3,6-DBSQ)(3,6-DBCat), and the average Co−N length of 1.998 Å is slightly shorter than the 2.026 Å length of the tmeda analogue.[4] Features of the two quinone ligands permit clear distinction between SQ and Cat. Oxygens O1 and O2 are associated with the SQ ligand as is evident from the C−O bond lengths (1.303(4) Å), the relatively long C1−C2 bond length (1.437(4) Å), and the contracted C3−C4 and C5−C6 bonds (1.367(5) Å). The Cat ligand, containing O3 and O4, has longer C−O lengths (1.347(4) Å) and aromatic C−C lengths for the ring. The N−Co−N bond angle for the tmmda ligand is 71.8(1)°, roughly 15° smaller than the angle within the five-membered tmeda chelate ring of Co^{III}(tmeda)(3,6-DBSQ)(3,6-DBCat).

Table 2. Selected Bond Lengths and Angles for Co^{III}(tmmda)(3,6-DBSQ)(3,6-DBCat) and Co^{II}(tmpda)(3,6-DBSQ)$_2$

	Co^{III}(tmmda)(3,6-DBSQ)-(3,6-DBCat)[a]	Co^{II}(tmpda)(3,6-DBSQ)$_2$	
		$T = 150$ K	$T = 298$ K
	Bond Lengths (Å)		
Co−O1	1.906(2)	2.040(6)	2.080(8)
Co−O2	1.864(2)	2.007(6)	2.025(8)
Co−O3	1.840(2)	2.021(7)	2.046(9)
Co−O4	1.863(2)	2.007(6)	2.012(9)
Co−N1	2.003(3)	2.180(10)	2.185(14)
Co−N2	1.993(3)	2.182(10)	2.210(14)
$C-O_{SQ}$	1.303(4)	1.287(12)	1.270(15)
$C-O_{Cat}$	1.347(4)		
	Angles (deg)		
O1−Co−O2	85.32(9)	81.0(2)	80.6(3)
O3−Co−O4	87.64(9)	81.1(3)	81.6(4)
N1−Co−N2	71.75(13)	95.0(4)	94.5(6)

[a] Oxygen atoms O1 and O2 of Co^{III}(tmmda)(3,6-DBSQ)(3,6-DBCat) belong to the semiquinonate ligand (Figure 1).

Magnetic data recorded for solid Co^{III}(tmmda)(3,6-DBSQ)(3,6-DBCat) confirm the Co(III) electron distribution at room temperature. The temperature dependence of the magnetic moment (Figure 2) shows that the complex remains as the $S = {}^1/_2$ redox isomer through the temperature range, converting to the high-spin Co^{II}(tmmda)(3,6-DBSQ)$_2$ isomer at temperatures above 350 K. This behavior is similar to Co(tmeda)(3,6-DBSQ)(3,6-DBCat) which undergoes transition to the Co(II) redox isomer within the same temperature range in the solid state.

The anisotropic EPR spectrum of Co^{III}(tmmda)(3,6-DBSQ)(3,6-DBCat) recorded in toluene at 77 K is shown in Figure 1S (Supporting Information). It consists of two components at g values of 2.0208 and 1.9998, each split into eight lines by coupling to the ^{59}Co ($I = {}^7/_2$) nucleus of 37 and 31 G, respectively. Weak anisotropy of the spectrum is consistent with its assignment as that of a localized semiquinone radical weakly coupled to the chelated metal.

Electronic spectra recorded for Co^{III}(tmmda)(3,6-DBSQ)(3,6-DBCat) in the solid state show intense absorptions at 645 and 2300 nm. DFT calculations by Noodleman and Hendrickson assign the 645 nm transition as a Co(dπ) → Q(π^*) transition and the low-energy band as a Cat → SQ transition between mixed charge ligands.[17] In toluene solution at 300 K, there is no observable λ_{max} at 650 nm, but there is an intense transition at 825 nm ($\epsilon = 2600$ M^{-1} cm^{-1}). This band is associated with the Co^{II}(tmmda)(3,6-DBSQ)$_2$ redox isomer. With a decrease in solution temperature to 180 K, the 645 nm ($\epsilon = 3300$ M^{-1} cm^{-1}) band appears with little residual intensity for the 825 nm transition (Figure 2S (Supporting Information)). Spectral changes in this region over the temperature range between 300 and 180 K indicate that the transition temperature for conversion between Co(III) and Co(II) redox isomers is 280 K, slightly below the $T_{1/2}$ for the related tmeda complex of 310 K.[4]

Co(tmpda)(3,6-DBQ)$_2$. Structural characterization on Co(tmpda)(3,6-DBQ)$_2$, carried out on a crystallographic data set collected at room temperature (298 K), gave a dramatically different result from the structure determinations on Co^{III}(tmmda)(3,6-DBSQ)(3,6-DBCat) and Co^{III}(tmmda)(3,6-DBSQ)(3,6-DBCat). Bond lengths to the metal were a clear indication

(16) Jung, O.-S.; Park, S. H.; Chae, H. K.; Sohn, Y. S. Manuscript in preparation.

(17) Adams, D. M.; Noodleman, L.; Hendrickson, D. N. *Inorg. Chem.* **1997**, *36*, 3966.

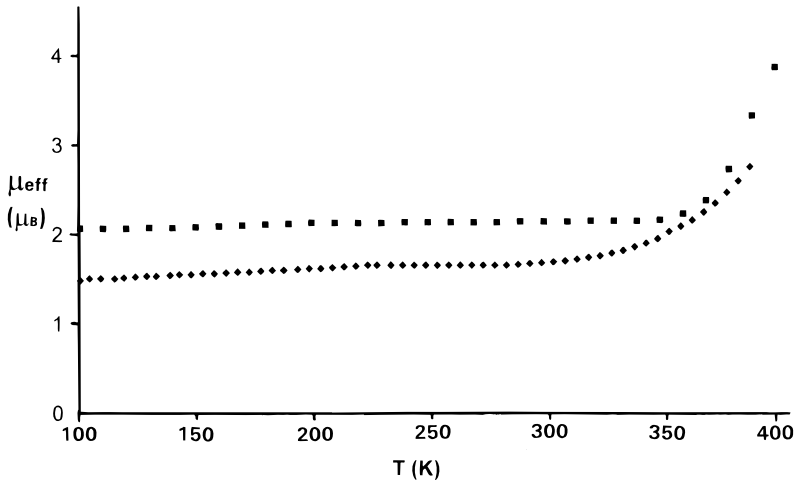

Figure 2. Magnetic measurements for Co(tmmda)(3,6-DBSQ)(3,6-DBCat) (■) and Co(tmeda)(3,6-DBSQ)(3,6-DBCat) (◆) in the solid state.

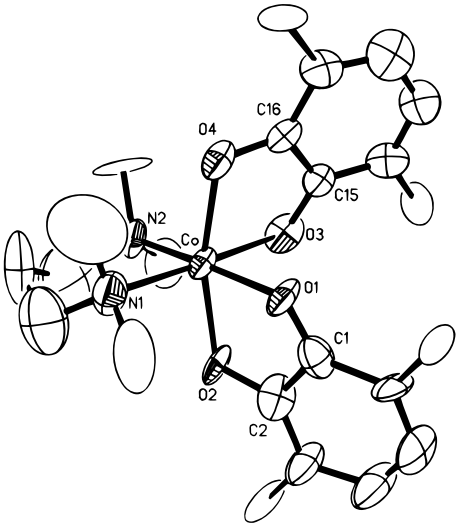

Figure 3. View of the Co^{II}(tmpda)(3,6-DBSQ)$_2$ molecule showing one location for the disordered tmpda carbon atoms.

of high-spin Co(II) for the Co^{II}(tmpda)(3,6-DBSQ)$_2$ redox isomer. The Co−O lengths average to 2.041 Å, the Co−N lengths average to 2.198 Å, and both values are roughly 0.2 Å longer than the average lengths to the tmmda and tmeda analogues. A view of the molecule is given in Figure 3; selected bond lengths and angles for structure determinations carried out at 298 K and at a lower temperature are listed in Table 2. Disorder in the tmpda ligand limited the precision of the structure determination at 298 K. Methyl and methylene carbon atoms bonded to nitrogen N1 were found to be ordered, but rotational disorder about the Co−N2 bond disordered the methyl groups bonded to N2 and resulted in conformational disorder for the remaining two methylene carbon atoms of the propylene bridge between N1 and N2. A second data set was collected on the crystal at a nozzle temperature of 150 K. In fact, with the results of magnetic characterization of the complex, it seems clear that the temperature at the crystal is somewhat above 150 K, but the low-temperature data set provided better resolution of the disordered atoms of the tmpda ligand. Bond lengths about the Co indicate that at the lower temperature the metal is still in the form of high-spin Co(II) and that the complex is the Co^{II}(tmpda)(3,6-DBSQ)$_2$ redox isomer. Features of the two quinone ligands indicate that they are both SQ. Lengths for the C−O bonds average to 1.287(12) Å, the average C−C bond length between quinone carbon atoms of the ring is 1.504(14) Å, and the pattern of C−C bond lengths within the ring shows contraction for the bonds that would be localized double bonds for the parent *o*-benzoquinone.

The results of magnetic measurements recorded for Co(tmpda)(3,6-DBQ)$_2$ in the solid state are shown in Figure 4. They show the transition from the $S = {}^1/_2$ Co^{III}(tmpda)(3,6-DBSQ)(3,6-DBCat) redox isomer that prevails on the low-temperature side of $T_{1/2}$ to the high-spin high-temperature form, Co^{II}(tmpda)(3,6-DBSQ)$_2$. The solid-state $T_{1/2}$ for Co(tmpda)(3,6-DBQ)$_2$ is 178 K in contrast with the solid-state $T_{1/2}$ values for Co(tmmda)(3,6-DBQ)$_2$ and Co(tmeda)(3,6-DBQ)$_2$ which are both above 350 K. At temperatures above 300 K the magnetic moment for Co^{II}(tmpda)(3,6-DBSQ)$_2$ is 5.7 μ_B, a value that approximates the magnetic moment for noninteracting hs-Co(II) and SQ radical centers. The EPR spectrum of Co^{III}(tmpda)(3,6-DBSQ)(3,6-DBCat) recorded in toluene glass at 77 K (Figure 1S) is similar to the spectrum obtained for the tmmda analogue showing that the shift to the Co(III) redox isomer occurs at low temperature. It consists of two components at $g_1 = 2.0180$ and $g_2 = 2.0019$, each split into eight lines by coupling the ^{59}Co nucleus with values of $A_1 = 35$ G and $A_2 = 30$ G. Electronic spectra recorded for Co(tmpda)(3,6-DBQ)$_2$ in the solid state show the temperature dependence that appears for the magnetic measurements. At 300 K, there is an intense transition at 845 nm associated with Co^{II}(tmpda)(3,6-DBSQ)$_2$. As temperature of the sample is decreased to 90 K, intense bands at 2500 and 650 nm appear with a decrease in intensity of the 845 nm transition. These bands are characteristic of Co^{III}(tmpda)(3,6-DBSQ)(3,6-DBCat). The 845 nm transition also appears for Co^{II}(tmpda)(3,6-DBSQ)$_2$ in toluene solution, but the transition to Co^{III}(tmpda)(3,6-DBSQ)(3,6-DBCat) occurs at a temperature below the freezing point of the solvent and the development of the Co(III) redox isomer has not been measured quantitatively in solution.

Valence Tautomerism for the Co(Me$_2$N(CH$_2$)$_n$NMe$_2$)(3,6-DBQ)$_2$ (n = 1−3) Series. Enthalpy and entropy changes, together, define the temperature range for the equilibrium between Co^{III}(Cat) and Co^{II}(SQ) redox isomers. The ancillary ligand chelate ring dimension is the differentiating feature for the members of the tmmda, tmeda, tmpda series. The unsaturated six-membered chelate ring of Co(tmpda) has greater conformational flexibility than the more contracted chelate rings of Co(tmmda) and Co(tmeda). Chelate ring flexibility for Co^{II}(tmpda)(3,6-DBSQ)$_2$ results in a relatively high transition temperature and conformational disorder in the X-ray structure. Magnetic measurements have been used to obtain thermody-

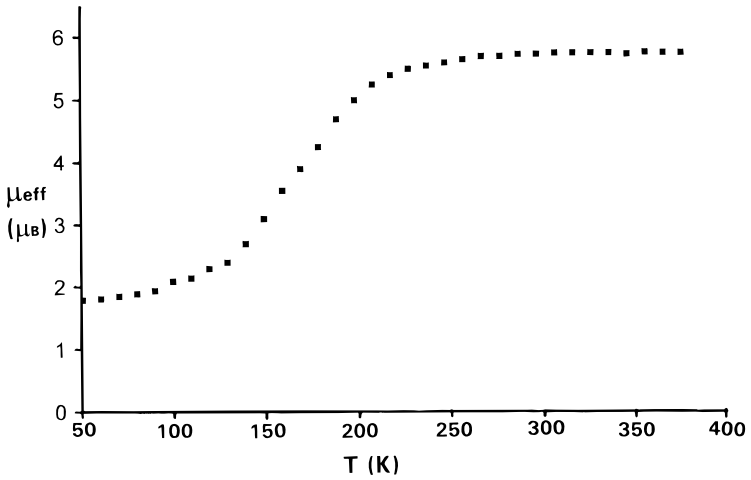

Figure 4. Changes in magnetic moment for Co(tmpda)(3,6-DBQ)$_2$ in the solid state with the transition from the Co(III) redox isomer at low temperature to the Co(II) isomer at temperatures above 178 K.

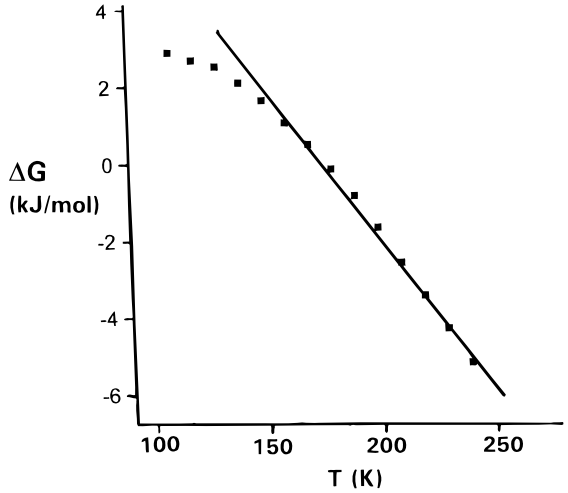

Figure 5. Plot of ΔG vs T for the Co^{III}(tmpda)(3,6-DBSQ)(3,6-DBCat)/Co^{II}(tmpda)(3,6-DBSQ)$_2$ equilibrium in the solid state.

namic parameters for the Co^{III}(Cat)/Co^{II}(SQ) equilibrium for Co(tmpda)(3,6-DBQ)$_2$ in the solid state. Magnetic data have been recorded at both increasing and decreasing temperature and show no significant hysteresis. Concentrations of the Co(III) and Co(II) redox isomers present at each temperature have been estimated from values of molar susceptibility,[10] and these values have been used to calculate K_{eq} and ΔG. The linear region of the plot of ΔG vs T, shown in Figure 5, has been used to obtain values of 14.2 kJ/mol for ΔH and 80 J/(mol K) for ΔS. Values of magnetic moment for the Co(III) and Co(II) redox isomers were 1.80 μ_B for Co^{III}(tmpda)(3,6-DBSQ)(3,6-DBCat) and 5.70 μ_B for Co^{II}(tmpda)(3,6-DBSQ)$_2$. A limit on the resolution of magnetic contributions for the two isomers results in nonlinearity for the plot shown in Figure 5 at temperatures much above and below the linear range used to calculate thermodynamic parameters.

While $T_{1/2}$ for Co(tmpda)(3,6-DBQ)$_2$ in the solid state is at an observable level, the values of both ΔH and ΔS are smaller than values reported for complexes containing bpy and phen ancillary ligands.[8,9] Hendrickson has estimated a minimum value for ΔS of 75 J/(mol K) for equilibria between Co^{III}(Cat) and Co^{II}(SQ) redox isomers on the basis of the ΔS_{elec} associated with the change in spin multiplicity and by using a value for ΔS_{vib} obtained from Fe(II) spin transition complexes.[7b] The ΔS obtained for the tmpda complex is only slightly larger than this value and substantially smaller than values obtained from magnetic measurements made in toluene solution that range from 118 to 134 J/(mol K) for the Co(N-N)(3,5-DBQ)$_2$ series, where N-N = bpy, dmbpy, and phen. A change in structure, from octahedral to trigonal prismatic, is an option open to the Co^{II}(N-N)(3,5-DBSQ)$_2$ redox isomers in solution, and structural isomerism contributes to the higher solution ΔS values.[4,16] In the rigid solid-state lattice, ΔS for Co(bpy)(3,5-DBQ)$_2$ decreases slightly to 98 J/(mol K).[8]

The shift in $T_{1/2}$ of approximately 150 deg between Co(tmeda)(3,6-DBQ)$_2$ and Co(tmpda)(3,6-DBQ)$_2$ with the addition of a single methylene group to the chelate ring is striking, and it emphasizes the extreme sensitivity of valence tautomeric equilibria to subtle changes in complex composition.

Spectral and magnetic measurements recorded for Co(tmmda)(3,6-DBQ)$_2$ and Co(tmeda)(3,6-DBQ)$_2$ have not provided a value for $T_{1/2}$ in the solid state due to the high temperature of transition. Spectral changes observed in toluene solution indicate that $T_{1/2}$ for the tmmda complex appears at 280 K, while for Co(tmeda)(3,6-DBQ)$_2$ the temperature is 310 K. These observations place the tmeda complex with the chelate ring of intermediate size as the member of the series with the highest $T_{1/2}$. Clearly effects other than chelate ring flexibility are important in defining transition temperature; for tmmda the contracted bite of the four-membered chelate ring may be important.

Conclusions. Equilibria between Co(N-N)(DBQ)$_2$ redox isomers are quite sensitive to electronic and entropic effects. Subtle changes in the nature of the N-donor ancillary ligand can result in dramatic changes in the temperature range for the equilibrium. This has been investigated for the saturated four-, five-, and six-membered chelate rings of the tmmda, tmeda, tmpda series. The six-membered chelate ring formed by the tmpda ligand has the greatest conformational flexibility, resulting in the lowest transition temperature for the series. Disorder in the Co(tmpda) region of Co(tmpda)(3,6-DBSQ)$_2$ in the solid state is a direct result of chelate-ring flexibility. Structural features of both Co(tmmda)(3,6-DBSQ)(3,6-DBCat) and Co(tmeda)(3,6-DBSQ)(3,6-DBCat) are ordered, and the transition temperature is approximately 150 deg higher with the more rigid chelate ring. For the pair of complexes, Co(tmeda)(3,6-DBSQ)(3,6-DBCat) has a slightly higher $T_{1/2}$, due, presumably, to the more contracted N−Co−N bite angle of the four-membered chelate ring, and the order of $T_{1/2}$ for the series is Co(tmeda) > Co(tmmda) ≫ Co(tmpda).

Acknowledgment. Research carried out at KIST was supported as part of the E-project through Grant 2N13694, and research at the University of Colorado was supported by the National Science Foundation.

Supporting Information Available: Tables listing detailed crystallographic data, atomic positional parameters, thermal parameters, and bond lengths and angles for Co^{III}(tmmda)(3,6-DBSQ)(3,6-DBCat) (T = 293 K) and Co^{II}(tmpda)$(3,6\text{-DBSQ})_2$ (T = 298 and 150 K), Figure 1S, showing EPR spectra of Co(tmmda)(3,6-DBSQ)(3,6-DBCat) (a) and Co(tmpda)(3,6-DBSQ)(3,6-DBCat) (b) obtained in toluene glass at 77 K, and Figure 2S, showing changes in intensity of the 650 nm transition of Co^{III}(tmmda)(3,6-DBSQ)(3,6-DBCat) ($c = 1.0 \times 10^{-4}$ M) and the 825 nm transition of Co^{II}(tmmda)$(3,6\text{-DBSQ})_2$ in toluene solution at 180, 230, 260, and 290 K (36 pages). Ordering information is given on any current masthead page.

IC9805372